Multi-modal Bike Sensing for Automatic Geo-annotation
Geo-annotation of Road/Terrain Type by Participatory Bike-sensing

Steven Verstockt[1], Viktor Slavkovikj[1], Pieterjan De Potter[1], Jürgen Slowack[2] and Rik Van de Walle[1]
[1]*Multimedia Lab – ELIS Department, Ghent University - iMinds,*
Gaston Crommenlaan 8, bus 201, Ledeberg-Ghent, Belgium
[2]*Barco NV, President Kennedypark 35, 8500 Kortrijk, Belgium*

Keywords: Multi-modal Sensing, Image Classification, Accelerometer Analysis, Geo-annotation, Mobile Vision, Machine Learning, Bike-sensing.

Abstract: This paper presents a novel road/terrain classification system based on the analysis of volunteered geographic information gathered by bikers. By ubiquitous collection of multi-sensor bike data, consisting of visual images, accelerometer information and GPS coordinates of the bikers' smartphone, the proposed system is able to distinguish between 6 different road/terrain types. In order to perform this classification task, the system employs a random decision forest (RDF), fed with a set of discriminative image and accelerometer features. For every instance of road (5 seconds), we extract these features and map the RDF result onto the GPS data of the users' smartphone. Finally, based on all the collected instances, we can annotate geographic maps with the road/terrain types and create a visualization of the route. The accuracy of the novel multi-modal bike sensing system for the 6-class road/terrain classification task is 92%. This result outperforms both the visual and accelerometer only classification, showing that the combination of both sensors is a win-win. For the 2-class on-road/off-road classification an accuracy of 97% is achieved, almost six percent above the state-of-the-art in this domain. Since these are the individual scores (measured on a single user/bike segment), the collaborative accuracy is expected to even further improve these results.

1 INTRODUCTION

Mobile phones have increasingly evolved in functionality, features and capability over the last decade. Nowadays, they are being used by many for more than just communication. With the continuous improvement in sensor technology built into these 'smartphones', and web services to aggregate and interpret the logged information, people are able to create, record, analyze and share information about their daily activities. As such, the mobile phone is well on its way to become a personal sensing platform (Goldman et al., 2009).

Within this mobile sensing (r)evolution, phone users acts as sensor operators, i.e., they contribute sensor measurements about their activities or the places they visit as part of a larger-scale effort to collect data about a population or a geographical area (Srivastava et al., 2012). This is the idea behind participatory or human-centric sensing. By combination of mobile data from large groups of individuals, it is possible to derive new values for end users in ways that the contributor of the content even did not plan or imagine and to perform functions that are either difficult to automate or expensive to implement.

Recently, the tendency of participatory data gathering has also started to occur in the domain of geographic information systems (GIS). Where the process of mapping the Earth has been the task of a small group of people (surveyors, cartographers, and geographers) for many years, it starts to become possible now for everyone to participate in several types of collaborative geographic projects, such as OpenStreetMap and RouteYou (Haklay and Weber, 2008). These projects are built upon user generated geographic content, so called volunteered geographic information (VGI). VGI makes it easier to create, combine, and share maps and supports the rapid production of geographic information. One drawback, however, is that a lot of the work still involves manual labor. Within our work we focus on how mobile sensors can help to automate and facilitate the more labor-intensive VGI tasks.

A common task performed by recreational GPS-

Verstockt S., Slavkovikj V., De Potter P., Slowack J. and Van de Walle R..
Multi-modal Bike Sensing for Automatic Geo-annotation - Geo-annotation of Road/Terrain Type by Participatory Bike-sensing.
DOI: 10.5220/0004531100390049
In *Proceedings of the 10th International Conference on Signal Processing and Multimedia Applications and 10th International Conference on Wireless Information Networks and Systems* (SIGMAP-2013), pages 39-49
ISBN: 978-989-8565-74-7

users is to find good routes in an area, where the quality of a route is mainly based on safety, efficiency, and enjoyment (Reddy et al., 2010a). From all the route characteristics, the road quality, i.e., the physical condition of the terrain, and the road/terrain surface showed to have a significant impact on how the users rank their routes. Currently, however, this information is largely unavailable. In order to bridge this gap, there is need for automatic road classification. Within this paper, we investigate the ability to determine the current road/terrain type from 'onboard' mobile sensors (i.e., from a smartphone mounted on a bike). Contrarily to manual VGI, our automatic approach facilitates real-time updates/annotation, e.g. when road conditions change or when new roads are found. Furthermore, by using common phones, it is not required to buy expensive, specialized sensing equipment, keeping the costs very low.

A general overview of the proposed setup is shown in Figure 1. Smartphone and GPS data are collected using the onboard device(s) mounted at the bike's handlebar. For the camera sensor, the terrain/road needs to be in the field-of-view of the camera. For the collection of the accelerometer data, the device can be placed or stored as wanted by the user. Based on the multi-sensor data, the road/terrain type is estimated using the novel multi-modal RDF-based classification algorithm, which is fed with a set of discriminative image and accelerometer features. Finally, a geographic map can be annotated automatically using this road/terrain information.

The remainder of this paper is organized as follows. Section 2 presents the related work in mobile-sensing for GIS road/terrain classification. Subsequently, Section 3 proposes our novel road/terrain classification method, based on accelerometer and visual features which are fed to the RDF. Next, Section 4 presents the experimental setup and discusses the data collection, ground truth (GT) creation and evaluation strategy/results. Finally, Section 5 ends this paper with conclusions.

2 RELATED WORK

Current mobile-sensing solutions for GIS road/terrain classification either use accelerometer data or visual images. Although they can easily (and successfully) be combined, the combination of both sensor types is not yet investigated.

Based on the observation that traversing different terrain types induces different vibration signals, Weiss et al., (2006) use an accelerometer mounted on a vehicle (i.e., a robot) to perform vibration-based road classification. To train and classify the vibration signals they fed a set of distinctive accelerometer features to a Support Vector Machine (SVM), which was shown to outperform alternative classification methods. Although they achieve around 80% correct classifications, the speed of the vehicle is not realistic (i.e., too slow) and the experiments were performed in a 'controlled' environment. The set of accelerometer features, however, is well-chosen and will (partly) be used in our set-up. A similar SVM-based approach is presented by Ward and Iagnemma (2009), where the algorithm is validated with experimental data collected with a passenger vehicle driving in real-world conditions. The algorithm is shown to classify multiple terrain types as correctly with 89%. However, they make use of expensive, specialized sensing equipment to achieve this accuracy and the classifier was only trained to recognize four very distinctive classes. When the classes vibration behavior would be closer to each other, e.g., when comparing tiles to cobblestones and asphalt to gravel, confusion of classes is expected to be higher, leading to lower accuracy. By using visual features, in addition to the accelerometer data, we are able to tackle this problem.

Tang and Breckon (2011) classify urban, rural and off-road terrains by analyzing several color and texture features (some are similar to ours). They report a performance of almost 90% correct classification on the road/off-road problem, also using SVM classification.

A drawback of the method of Tang and Breckon, however, is the genericity of the on-/off-road classes, i.e., too broad for recreational purposes, and the strict positioning of the camera zones. Similar limitations arise in (Popescu et al., 2008). Interesting, however, is that these authors split up the image into small regions and perform a 'voting' over these regions. In this way, conflicting or confusing zones can (probably) be detected and eliminated, leading to higher classification accuracy. Furthermore, it is also important to mention that the majority of the visual classification approaches use an 'unrealistic' set-up, i.e., sharp images containing a single terrain type captured from a perpendicular camera angle. Our approach, on the opposite, uses images from real bike runs, containing blurred images with non-sharp terrain boundaries. As such our accuracy of 92% is a 'real-life' accuracy.

Although SVM has shown to perform best in the majority of the related work, Khan et al., (2011) recently showed that Random Decision Forests

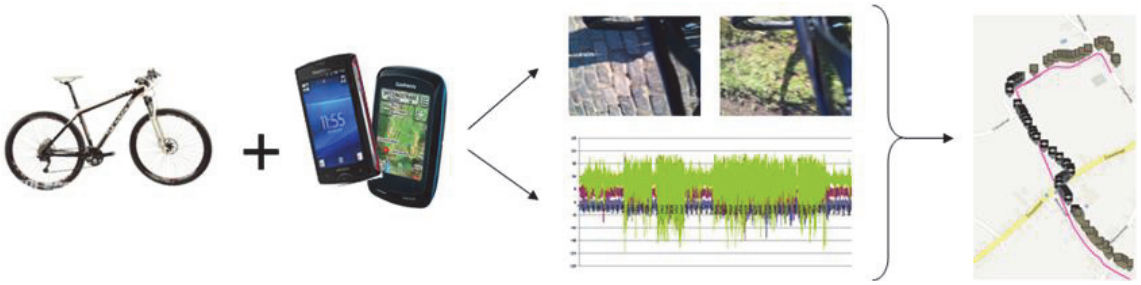

Figure 1: General overview of the multi-modal bike sensing setup.

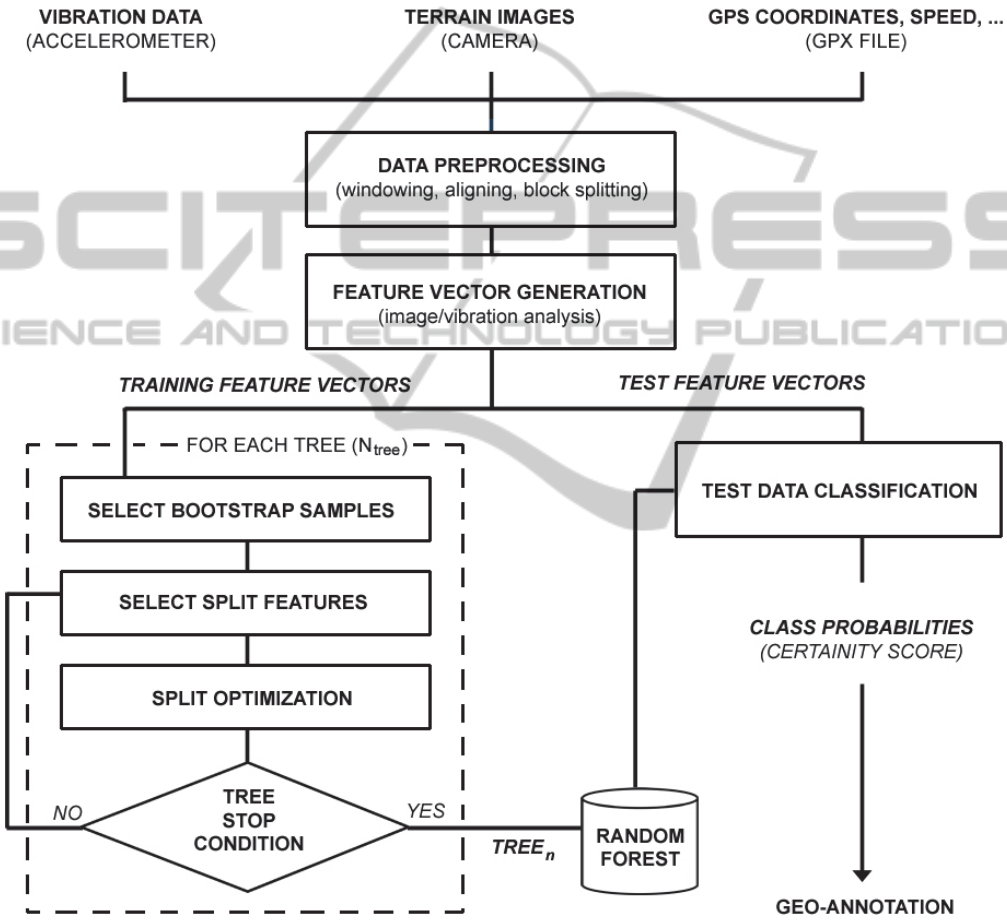

Figure 2: Multi-sensor RDF-based terrain classification.

(RDF) improve the SVM results in the context of road/terrain classification. This hypothesis was also confirmed by SVM-RDF comparisons performed on our experimental data. A gain of 7% was achieved when using RDF instead of SVM for visual classification. For accelerometer classification, the gain was lower, however, still 2%. As such, RDF, which is an ensemble classifier consisting of a collection of individual decision tree predictors, is used in our work. As an alternative, Relevance Vector Machines (RVM) are also gaining importance (Yogameena et al., 2010). RVM yields a formulation similar to SVM with probabilistic classification similar to RDF. In future research, we will study its performance in terrain classification.

3 MULTI-SENSOR TERRAIN CLASSIFICATION

The multi-modal bike sensing system is built upon

three sensing components: an accelerometer, a digital camera, and a GPS. Each of these sensors independently and concurrently captures surface terrain data. Based on this multi-modal data, the proposed terrain classification system tries to estimate which type of terrain (asphalt, cobblestones, tiles, gravel, grass, and mud) the vehicle is currently traversing.

A general scheme of the classification system is shown in Figure 2. First, the raw sensor data is pre-processed. The windowing groups the vibration data into overlapping data fragments of 5 seconds and aligns them onto the corresponding images and the GPS data. The images are also split into blocks in order to detect/eliminate conflicting or confusing zones, as in the work of Popescu et al., (2008). Subsequently, we further process/analyze the sensor data to create a set of training and test feature vectors (which is discussed in detail in Section 3.1). Next, the training vectors are used to construct a random forest of binary decision trees (as explained in Section 3.2). Finally, the test vectors are classified using the trained RDF. Based on the RDF class probabilities and the corresponding GPS data, geo-annotation of test data can be performed.

3.1 Feature Extraction

For each of the sensor data segments, i.e., for each 5 seconds of biking, we extract a set of discriminative visual and vibration features which best describe the road/terrain conditions. The selection of these features is based on the state-of-the-art (SOTA) study (discussed in Section 2), and on our test data evaluation (~Section 4). When features show a similar behaviour, the feature with lowest computational cost is chosen.

3.1.1 Accelerometer/Vibration Features

Figure 3 shows some samples of the accelerometer readings for the different road/terrain types. It is easy to see that not every road type does have a distinct pattern, e.g., the differences between tiles and grass are limited. Similar 'feature equalities' occur in the visual domain, however, not between the same pairs of road/terrain types. As such, by performing a multi-modal analysis it is expected that the ambiguities in the vibration data can be compensated by the visual data, and vice versa.

The accelerometer of our mobile device(s) detects the vibration along the X, Y and Z-axes (see Figure 3). Important to remark is that, depending on the position of the device, $\{x,y,z\}$ coordinates will vary and will complicate the classification task. In order to overcome this obstacle, of forcing the user to place the device in a pre-defined position, the magnitude m of the acceleration is calculated:

$$m = \sqrt{x^2 + y^2 + z^2} \quad (1)$$

Computing (and analyzing) the features on the vibration magnitude m, instead of on the individual accelerometer data along the X, Y and Z-axes, enables our system to assume a random and possibly changing orientation for the mobile device, i.e., increases the user's freedom.

The set of features which were found to best describe the bike vibrations are a combination of the once proposed in (Weiss et al., 2006) and (Reddy et al., 2010b), and are defined as follows:

- $\mu(m)$: mean of m – for flatter/smoother surfaces (e.g. asphalt), $\mu(m)$is low (close to 0).
- $max(m)$: maximum of m – takes large values for terrain types that contain big bumps, e.g., cobblestones and grass/mud.
- $min(m)$: minimum of m – takes larger values for flat terrains (e.g., asphalt).
- $\sigma(m)$: standard deviation of m – is higher for coarse terrain types (e.g., gravel) than for smoother ones (such as tiles and asphalt).
- $\|m\|$: norm of m – is large if the acceleration is constantly high, as it is for cobblestones.
- $E(m)$: energy, i.e., squared FFT sum of m (Ravi, 2005) – takes larger values for coarse terrain types, such as grass, mud and gravel.

It is important to remark that each of these vibration features is calculated over a sliding overlapping time window of 5 seconds, in order to align them with the visual features which are discussed hereafter. A similar windowing approach has demonstrated success in previous work (Bao and Intille, 2004).

Table 1: Exemplary accelerometer features for each of the investigated terrain types.

	asphalt	cobble-stones	tiles	grass	mud	gravel
$\mu(m)$	9.811	10.777	10.248	11.274	10.899	9.121
$max(m)$	12.904	27.692	19.193	21.781	18.495	17.036
$min(m)$	6.749	1.909	3.201	1.916	4.022	3.294
$\sigma(m)$	1.139	4.185	3.559	4.537	3.284	3.050
$\|\| m \|\|$	108	129	120	135	126	107
$E(m)$	11705	16556	14463	18144	15927	11461

Table 1 shows exemplary accelerometer feature values for each of the investigated terrain types. This

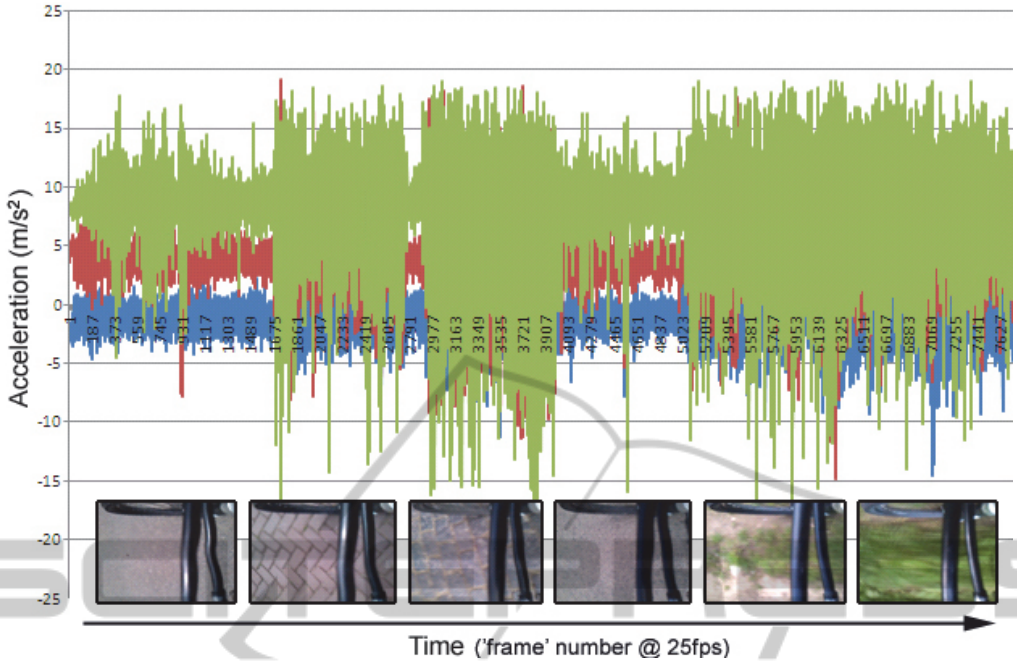

Figure 3: Exemplary accelerometer data along the X, Y and Z-axes. Visual images of corresponding terrain types are shown below the graph.

makes clearer the relation between each of the features and the road/off-road terrain types.

3.1.2 Visual Features

Some of the investigated terrain types are hard to recognize using an accelerometer (see evaluation results - Section 4). Since these terrains have similar vibration behaviour, it is not always possible to distinguish between their feature values. Visual features can help to overcome these problems. The other way around, accelerometer features can help to cope with (possible) visual ambiguities. Multi-modal combination of visual and vibration features is, as such, a win-win.

The set of visual features that has been found to be most appropriate for the terrain classification task, consists of color-, texture-, edge- and energy-based measures. In total, 8 features are used (each of them calculated on the camera image `I`). They are defined as follows:

- `blue(I)`: percentage 'blue' pixels based on HSV-blue range – for cobblestones and asphalt, for example, `blue(I)` is close to 1.
- `green(I)`: histogram spread of 'green' HSV pixels – takes large values for grass.
- `mud(I)`: percentage low-saturated 'orange-red' HSV pixels – is large for mud and some types of brown colored gravel.
- `gray(I)`: percentage pixels that meet the gray RGB equality criteria (i.e., R ≈ G ≈B) - is higher for road types (e.g., asphalt and cobblestones) than for off-road ones (such as grass and gravel).
- *E*`(I)`: FFT energy spread of `I` – is large if the terrain image has a lot of high energy texture, as it is for grass and cobblestones.
- *Hough*`(I)`: Hough Transform based number of distinct edge directions in `I` – is only high for tiles and cobblestones.
- *EOH*`(I)`: MPEG-7 Edge Orientation Histogram based spread of edges in `I` (Pinheiro, 2009) - takes large values for terrain types with random edge distribution, such as grass and gravel.
- *GLCM*`(I)`: Product of gray-level co-occurence matrix (Ershad, 2011) statistics of local binary pattern (Pietikäinen et al.,) filtered image of `I` – is high for cobblestones and off-road terrains.

Similar to the accelerometer features in Table 1, Table 2 shows exemplary visual feature values for each of the investigated terrain types. This makes clearer the relation between each of the visual features and the road/off-road terrain types and also shows the 'feature equalities' in vibration and visual domain, e.g., the *GLCM*`(I)` - μ`(m)` similarity.

After generation of the visual and vibration features, they are divided into training and testing vectors. The training vectors are used to construct a

random forest of binary decision trees (discussed hereafter). The test vectors will be evaluated using this RDF classifier, in order to retrieve the accuracy of the overall terrain classification system.

Table 2: Exemplary visual features for each of the investigated terrain types.

	asphalt	cobble-stones	tiles	grass	mud	gravel
blue(I)	0.823	0.929	0.879	0.159	0.131	0.706
green(I)	1	7	17	88	12	9
mud(I)	0.037	0.113	0.207	0.152	0.833	0.256
gray(I)	0.944	0.826	0.766	0.282	0.695	0.685
E(I)	0.292	0.739	0.257	0.43	0.26	0.276
Hough(I)	0	13	12	2	0	0
EOH(I)	1.007	1.550	2.010	1.622	2.211	1.502
GLCM(I)	0.068	2.740	3.072	2.769	2.202	0.360

3.2 RDF Classification

Random Decision Forests (RDF) is a very fast tool for classification and clustering, which has shown to be extremely flexible in the context of computer vision (Gall et al., 2012). The most known application of RDF is the detection of human body parts from depth data in the Microsoft KINECT (Shotton, 2011). This commercial application demonstrates the practicability of RDF for large-scale real-world computer vision problems.

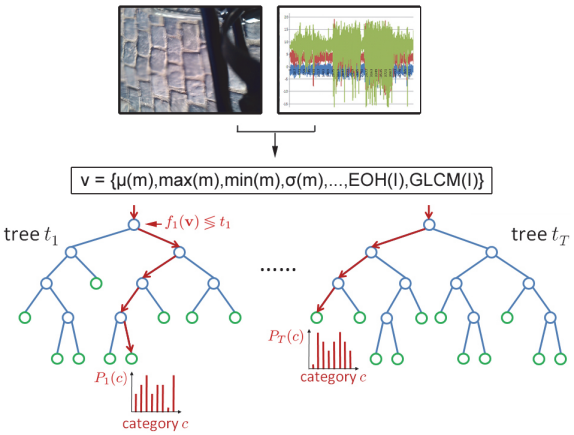

Figure 4: The random forest consists of a set of trees that map the multi-modal feature vector v to a distribution Pi(c) stored at each leaf. The disks indicate split nodes that evaluate one of the features of v and pass it to the right/left child until a leaf is reached (Shotton et al., 2009).

The accuracy of RDF is comparable with other classifiers. Furthermore, Khan et al., (2011) recently showed that RDF improves SVM in terrain classification tasks. Other advantages of RDF are its simple training and testing algorithms, and the fact that is can easily perform multi-class classifications.

Random forests are ensembles of randomized decision trees T_n, as illustrated in Figure 4. Each of the N_{tree} trees consists of split nodes and leaves which map the multi-modal feature vector v to a distribution $P_i(c)$ stored at each leaf. The split nodes evaluate the arriving feature vector and depending on the feature values, pass it to the left or right child. Each leaf stores the statistics of the training vectors. For a classification task, it is the probability for each class c, denoted by $P(c|v)$:

$$P(c \mid v) = \sum_{n=1}^{N_{tree}} P_n(c \mid v) \quad (2)$$

For a more general discussion on random forests, we refer to the book of Breiman (2001) and the tutorial of Shotton et al., (2009).

4 EXPERIMENTAL SETUP AND EVALUATION RESULTS

In order to evaluate the proposed architecture we have performed several bike tours. During these tours we collected the training/test data and annotated them with the ground truth (GT). Based on this GT, we evaluated the test data while varying the number of trees (N_{tree}) and the sample ratio r (i.e., the percentage randomized training vectors used in each tree construction). Recently, we have also launched a bike app (shown in Figure 5) to extensively test the proposed set-up and collect more test data. Further development/testing will be performed on the user collected field data.

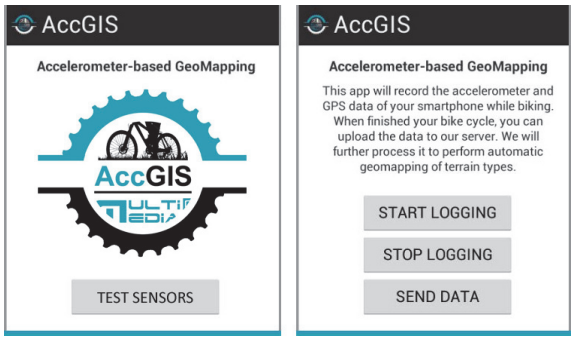

Figure 5: Accelerometer-based GeoMapping bike app.

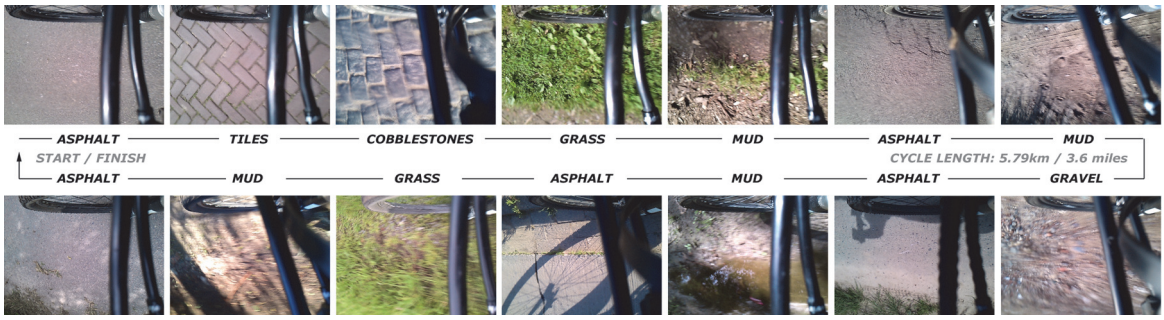

Figure 6: Exemplary bike cycle (start = finish).

4.1 Data Collection

The data collection was performed using standard 26'' and 29'' mountain bikes. Multiple cycles with varying terrain conditions (in type and frequency) were performed in several rural and (sub)urban regions all over Belgium. An exemplary run, in which all 6 terrain types occurred, is shown in Figure 6. In order to have varying weather conditions, the cycle runs were spread over the year, both in winter and summer on sunny and rainy days. Furthermore, tyre pressure and tyre types were changed in between several runs in order to cope with the tyre-vibration dependency.

To collect the vibration, visual and GPS data we used a Sony Ericsson Xperia mini Android smartphone and a Garmin Edge 800 bike GPS. On the smartphone we ran an accelerometer data logger and the time lapse android app, which takes a picture each five seconds. The bike GPS collected all geographical data and bike statistics. Based on the timestamps, which are stored for each sensor reading, the sensor data is aligned on each other.

The data was processed and analyzed on a standard PC with an Intel Pentium IV 2.4 GHz processor. The current version of the software is written in C# using the open source AlgLib data processing framework (http://www.alglib.net/) and the Emgu CV (http://www.emgu.com/) image processing library (for RDF classification and visual analysis respectively).

4.2 Ground Truth Creation

The ground truth creation is performed by visual analysis of the terrain images using a custom built ground-truth marking application. In addition to this image-based annotation, we also extend the GT with the available geographic terrain data of online maps. This data can be retrieved by reverse geocoding of the GPX latitude / longitude information of our GPS.

As can be seen in the cycle run in Figure 6, it is not always clear / easy to distinguish between some of the off-road types. Sometimes, the terrain consists of a combination of multiple terrain types, e.g., grass and mud, or gravel and mud. In these situations, ground truth annotation is difficult and can be error-prone. A similar kind of ground-truth inaccuracy was also reported in (Strazdins, 2011). In order to cope with this GT issue, we will extend the GT concept to allow multi-annotation. Currently, one can also discard these misclassifications from the confusion matrices and other evaluation metrics, which are discussed hereafter.

4.3 Evaluation Strategy / Metrics

First of all, it is important to mention that both 6-class and 2-class road/off-road classifications are evaluated. This facilitates comparison with SOTA works, which mainly perform 2-class classification or not always use the same set of terrain types. Furthermore, depending the application in which the classification system is used, the degree of specificity will also differ, i.e., for some GIS tools a road/off-road discrimination is sufficient.

The accuracy of the proposed system is evaluated for increasing number of RDF trees (N_{tree}) and increasing sample ratio r (which is related to the number of bootstrap samples). We define the accuracy as the proportion of the total number of predictions that were correct, i.e., the ratio of the number of correctly classified test vectors and the total number of test vectors. This accuracy will be calculated for each of the sensors individually, i.e., the visual and accelerometer accuracy, and also for their combination, i.e., the multi-modal accuracy. When they are combined, we use a winner-take-all strategy, where the sensor with the highest class probability in $P(c|v)$ wins. Other 'merging' strategies were also investigated, however, not leading to better multi-modal accuracy results.

Like in the work of (Khan et al., 2012), the evaluation is performed using 10-fold cross-validation. The data collected during our bike cycles is randomly divided into ten equal-sized pieces. Each piece is used as the test set with training done on remaining 90% of the data. The test results are then averaged over the ten cases, i.e., the accuracies that are reported are the average accuracy over 10 RDF runs.

In order to allow a more detailed analysis, we also generated confusion matrices (Kohavi and Provost, 1998) for the optimal RDF N_{tree}–r combinations. These matrices contain information about the actual (~ GT) and predicted classifications done by a classification system and report the number of false positives (FP), false negatives (FN), true positives (TP), and true negatives (TN). The strength of a confusion matrix is that it identifies the nature of the classification errors, as well as their quantities.

4.4 Results

First, we will present the accuracy results for each of the sensors individually, i.e., the accelerometer and visual accuracy. Subsequently, we will present their multi-modal accuracy, based on the winner-take-all strategy. The graphs (Graph 1-6) show the accuracy for increasing number of RDF trees (N_{tree}) and increasing sample ratio r. Both 6-class and road/off-road 2-class accuracy are shown.

Similar to (Ravi, 2005), we also performed leave-one-out feature evaluation, in order to find out which features among the selected ones are less important than the others. We ran the RDF classification with one attribute removed at a time. The $E(I)$ and $\|m\|$ features turn out to be the least significant. Leaving them out, however, leads to a significant change of 2-3% in accuracy, i.e., a trade-off between accuracy and computational complexity.

In general, each of the terrain types were classified correctly to a high degree, but also some misclassifications occurred. From these misdetections, mud and grass were mostly confused with each other. As discussed in Section 4.2, however, this can also be caused due to some ground-truth inaccuracy in the case of multi-class terrain images.

Finally, it is also important to remark that the visual accuracy is based on an optimal positioning of the smartphone camera. It the camera is not placed facing down as in our setup, we expect the visual accuracy to be some percentages lower. Future work will investigate the impact of the sensor positioning.

4.4.1 Accelerometer/Vibration Results

Graph 1 shows the accuracy for the 6-class terrain classification solely based on accelerometer data. For an optimal RDF configuration ($N_{tree}\approx32$; $r\approx0.65$), an accuracy of 71% is achieved. For 2-class road/off-road classification, the accuracy is 87%, as can be seen in Graph 2. Since these are the 'individual' accuracy scores (measured on a single user/bike segment), the collaborative accuracy is expected to even further improve these results. As such, accelerometer-only classification can even be used with high accuracy within our system, for example, when visual data is not available.

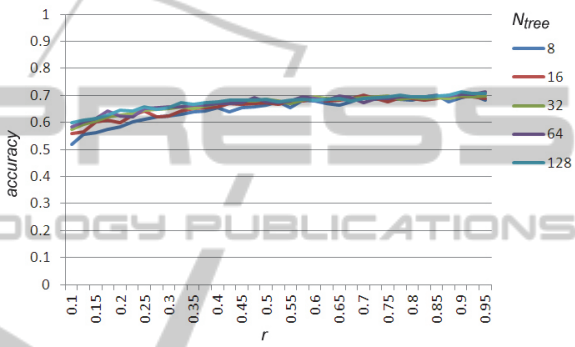

Graph 1: Accuracy of ***6-class terrain classification*** solely based on ***accelerometer data***. Results are shown for increasing number of RDF trees (N_{tree}) and increasing sample ratio r.

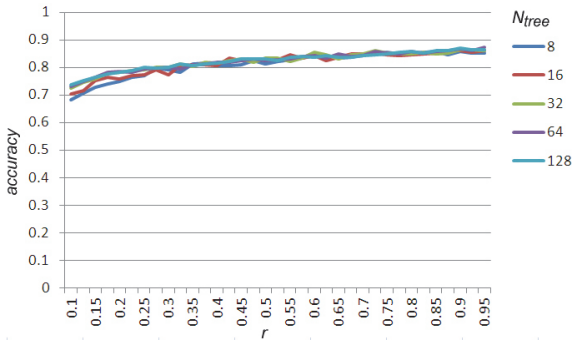

Graph 2: Accuracy of ***2-class road/off-road terrain classification*** solely based on ***accelerometer data***. Results are shown for increasing number of RDF trees (N_{tree}) and increasing sample ratio r.

4.4.2 Visual Results

Graph 3 shows the accuracy for the 6-class terrain classification solely based on visual data. For an optimal RDF configuration (Ntree≈32; r≈0.60), an accuracy of 90% is achieved.

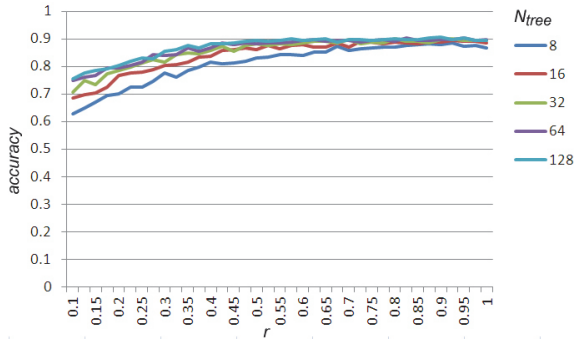

Graph 3: Accuracy of ***6-class terrain classification*** solely based on ***visual data***. Results are shown for increasing N_{tree} and r.

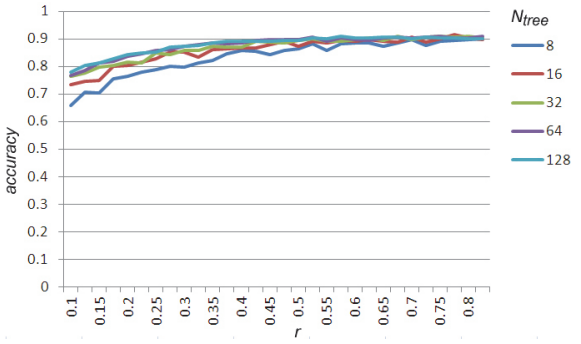

Graph 5: Accuracy of ***6-class terrain classification*** based on ***multi-modal visual-accelerometer data***. Results are shown for increasing N_{tree} and r.

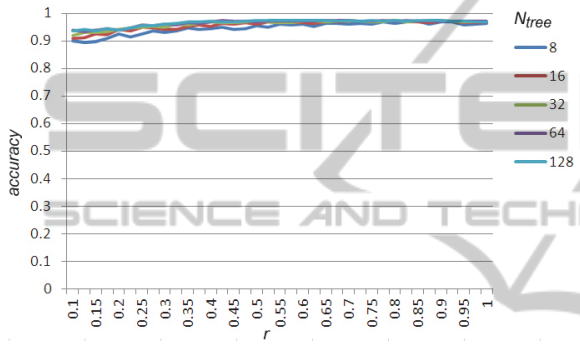

Graph 4: Accuracy of ***2-class road/off-road terrain classification*** solely based on ***visual data***. Results are shown for increasing N_{tree} and r.

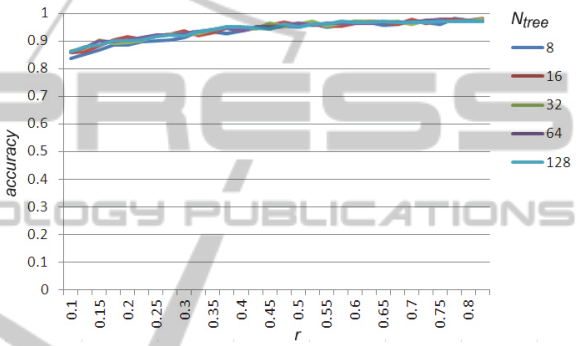

Graph 6: Accuracy of ***2-class road/off-road terrain classification*** based on ***multi-modal visual-accelerometer data***. Results are shown for increasing N_{tree} and r.

For 2-class road/off-road classification, the 'visual-only' accuracy is 96%, as can be seen in Graph 4. Again we remark that this visual accuracy is based on an optimal positioning of the smartphone camera. Due to this optimal positioning, the gain of multi-modal analysis is not that big (less than 2%), as discussed hereafter. However, since the accuracy of visual analysis will not always be so high in real-life conditions, it is safe to state that the multi-modal approach outperforms both the accelerometer and visual-only terrain classification.

4.4.3 Combined 'Multi-modal' Results

Graph 5 shows the accuracy for the 6-class terrain classification based on both visual and accelerometer data. For an optimal RDF configuration ($N_{tree} \approx 64$; $r \approx 0.55$), an accuracy of almost 92% is achieved (based on winner-take-all strategy). For 2-class road/off-road classification, the multi-modal accuracy is 97% (see Graph 6). Both results show that our system outperforms the SOTA work in this domain (discussed in Section 2).

4.4.4 Confusion Matrices

Figure 7 shows the visual and accelerometer confusion matrices for their optimal RDF N_{tree}–r combinations. As the visual confusion matrix in Figure 7a shows, each of the terrain types was classified correctly to a high degree. Only a limited number of misclassifications occurred, mostly mud and grass being confused with each other. For the accelerometer classification (shown in Figure 7b), most misdetections occur on off-road terrain types.

	A	C	T	G	M	Gr
A	037	000	000	001	000	000
C	002	038	000	000	000	000
T	001	001	038	000	001	000
G	000	000	000	032	004	000
M	000	000	002	006	034	000
Gr	000	001	000	001	001	040

a) visual confusion matrix

	A	C	T	G	M	Gr
A	039	000	000	001	000	002
C	000	035	000	008	006	000
T	000	000	039	006	002	006
G	001	001	001	013	005	004
M	000	004	000	005	021	006
Gr	000	000	000	007	006	022

b) accelerometer confusion matrix

Figure 7: Confusion matrices.

5 CONCLUSIONS

In this paper, we have presented the detailed design, implementation and evaluation of a novel road/terrain classification system. The proposed system shows how mobile sensors can help to automate and facilitate some of the more labor intensive VGI tasks. Based on the analysis of volunteered geographic information gathered by bikers, geographic maps can be annotated automatically with each of the 6 terrain types: asphalt, cobblestones, tiles, gravel, grass, and mud.

In order to perform the terrain classification task, the system employs a random decision forest (RDF), fed with a set of discriminative image and accelerometer features. The multi-sensor terrain classification achieves 92% accuracy for the 6-class terrain classification problem, and 97% accuracy for the on-/off-road classification. Since the evaluation is performed on data gathered during real bike runs, these are 'real-life' accuracies.

Future work will focus on the influence of bike conditions (e.g., speed and ascent/descent) on the classification results. If someone is biking faster, for example, it is expected that the accelerometer will be more discriminative, while for slower bikers, visual features will (probably) be. Further research is needed to check these hypotheses and to incorporate these kinds of dependencies in our system. Finally, when no visual data is available, for example when the camera is blocked or not facing the terrain, we also think of using reverse geocoding techniques to query and analyze online geographic data.

ACKNOWLEDGEMENTS

The research activities as described in this paper were funded by Ghent University, iMinds, University College West Flanders, the Institute for the Promotion of Innovation by Science and Technology in Flanders (IWT), the Fund for Scientific Research-Flanders (FWO-Flanders), the Belgian Federal Science Policy Office, and the EU.

REFERENCES

Bao, L. & Intille, S. S., 2004. Activity recognition from user-annotated acceleration data, In Pervasive Computing, Vol. 3001, pp. 1-17.

Breiman, L., 2001. Random forests. In Machine Learning, Vol. 45, No. 1, pp. 5-32 (2001)

Ershad, S. F., 2011. Texture Classification Approach Based on Combination of Edge & Co-occurrence and Local Binary Pattern, In *Proceedings of International Conference on Image Processing, Computer Vision, and Pattern Recognition*, pp. 626-629.

Gall, J., Razavi, N. & Van Gool, L., 2012. An Introduction to Random Forests for Multi-class Object Detection, In *LNCS Outdoor and Large-Scale Real-World Scene Analysis*, Vol. 7474, pp 243-263.

Goldman, J., Shilton, K., Burke, J., Estrin, D., Hansen, M., Ramanathan, N., Reddy, S., Samanta, V., Srivastava, M. & West, R., 2009. Participatory Sensing - A citizen-powered approach to illuminating the patterns that shape our world. In *White paper of Woodrow Wilson International Center for Scholars – Foresight and Governance project*.

Haklay, M. & Weber, P., 2008. OpenStreetMap:User-Generated Street Maps, In *Pervasive Computing*, Vol. 7, No. 4, pp. 12-18.

Khan, Y. N., Komma, P., Bohlmann, K. & Zell, A., 2011. Grid-based Visual Terrain Classification for Outdoor Robots using Local Features, In *IEEE Symposium on Computational Intelligence in Vehicles and Transportation Systems (CIVTS 2011)*, pp. 16-22.

Khan, Y. N., Masselli, A. & Zell, A., 2012. Visual Terrain Classification by Flying Robots, In *IEEE International Conference on Robotics and Automation (ICRA 2012)*, pp. 498 – 503.

Kohavi R. & Provost, F., 1998. Glossary of terms, In Machine Learning, Vol. 30, pp. 271-274.

Pietikäinen, M., Hadid, A., Zhao, G. &Ahonen, T., 2011. Computer Vision Using Local Binary Patterns, In *Computational Imaging and Vision*, Vol. 40.

Pinheiro, A. M. G., 2009. Image Descriptors Based on the Edge Orientation, In *Proceedings of the 4th International Workshop on Semantic Media Adaptation and Personalization*, pp. 73-78.

Popescu, D., Dobrescu, R. & Merezeanu, D., 2008. Road Analysis based on Texture Similarity Evaluation, In *Proceedings of the 7th WSEAS International Conference on Signal Processing (SIP'08)*, pp. 47-51.

Ravi, N., Dandekar, N., Mysore, P. & Littman, M.L., 2005. Activity Recognition from Accelerometer Data, In *Proceedings of the 17th Conference on Innovative Applications of Artificial Intelligence*, pp. 1541-1546.

Reddy, S., Shilton, K., Denisov, G., Cenizal, C., Estrin, D. & Srivastava, M., 2010a. Biketastic: Sensing and Mapping for Better Biking, In *Proceedings of the SIGCHI Conference on Human Factors in Computing Systems (CHI'10)*, pp. 1817-1820.

Reddy, S., Mun, M., Burke, J., Estrin, D., Hansen M. & Srivastava, M., 2010b. Using Mobile Phones to Determine Transportation Modes, In *Transactions on Sensor Networks*, Vol. 6, No. 2, pp. 13:1-27.

Srivastava, M., Abdelzaher, T. & Szymanski, B., 2012. Human-centric Sensing, In *Philosophical Transactions of Royal Society*, Vol. 370, No. 1958, pp. 176-197.

Shotton, J, Kim, T.-K. & Stenger, B., 2009. Boosting & Randomized Forests for Visual Recognition (tutorial), In *International Conference on Computer Vision*.

Shotton, J., Fitzgibbon, A., Cook, M., Sharp, T., Finocchio, M., Moore, R., Kipman, A. & Blake, A., 2011. Real-time human pose recognition in parts from single depth images, In *IEEE Conference on Computer Vision and Pattern Recognition*, pp. 1-8.

Strazdins, G., Mednis, A., Zviedris, R., Kanonirs, G. & Selavo, L., 2011. Virtual Ground Truth in Vehicular Sensing Experiments: How to Mark it Accurately, In *Proceedings of 5th International Conference on Sensor Technologies and Applications (SENSORCOMM 2011)*, pp. 295-300.

Tang, I. & Breckon, T. P., 2011. Automatic Road Environment Classification, In *Trans. on Intelligent Transportation Systems*, Vol. 12, No. 2, pp. 476-484.

Yogameena, B., Lakshmi, S. V., Archana, M. & Abhaikumar, S. R., 2010. Human Behavior Classification Using Multi-Class Relevance Vector Machine, In Journal of Computer Science, Vol. 6, No. 9, pp. 1021-1026.

Ward, C. C. & Iagnemma, K., 2009. Speed-independent vibration-based terrain classification for passenger vehicles, In *Vehicle System Dynamics*, Vol. 47, No. 9, pp. 1095–1113.

Weiss, C., Frohlich, H. & Zell, A., 2006. Vibration-based Terrain Classification Using Support Vector Machines, In *Proceedings of the 2006 IEEE/RSJ International Conference on Intelligent Robots and Systems (IROS)*, pp. 4429-4434.